JMC Publication
SINCE 1951

JOAASR
Journal of Advanced Applied Scientific Research

Original Research Paper **JOAASR-Vol-3-1 January** 2021: 7-15

Magnesium and zinc diffused growth and characterization of strontium L(+) tartrate pentahydrate crystals

K. B. Reema[1,2], N. Jagannatha[1*], K. P. Nagaraja[1], Delma D'Souza[1]

[1] *PG department of Physics, FMKMC College (A constituent college of Mangalore university), Madikeri-571201, Karnataka, India.*
[2] *Department of Physics, Maharani's Science College for Women (Affiliated to Mysore University), Mysuru-570005, Karnataka, India.*

Abstract:

Single crystals of intrinsic strontium L(+) tartrate (IST), Mg^{2+} doped strontium L(+) tartrate (MDST) and Zn^{2+} doped strontium L(+) tartrate (ZDST) are grown using gel diffusion method. Optimum condition for crystal growth is established by varying density of Sodium Meta Silicate (SMS) solution, gel pH, concentration and matrix of supernatant solutions. Stoichiometric composition and cationic distribution of the grown crystals are analyzed by EDAX measurements. Fourier transform infrared (FTIR) and Laser Raman spectral studies unveil various functional groups in the grown crystals. Thermo gravimetric analysis (TGA) confirms the presence of water molecules in the lattices and reveals decomposition behavior of the crystals in the temperature range of 30-1000 ^{o}C. Experimental data are used to generate the chemical formula for IST, MDST and ZDST crystals. IST crystals are found to possess a chemical formula: $SrC_4H_4O_6.5H_2O$ with a molecular weight of 325.77. MDST crystals show up with a chemical formula of $Sr_{0.9987}Mg_{0.0013}C_4H_4O_6.5H_2O$ (molecular weight 325.69) having a cationic distribution ratio: Sr^{2+}:Mg^{2+}=768:1. The ZDST crystal bears a chemical formula of $Sr_{0.9929}Zn_{0.0071}C_4H_4O_6.5H_2O$ (molecular weight 325.61) with a cationic distribution ratio: Sr^{2+}:Zn^{2+}=140:1. During the final stage of decomposition at high temperatures (761-1000 ^{o}C), the parent IST and the doped MDST and ZDST crystals attain stable state and exhibit thermal stability indicating usefulness of these crystals in high temperature electronics

Keywords: doped strontium tartrate, DSC, FTIR, gel technique, intrinsic strontium tartrate, Raman, TGA

*Corresponding author Email: jagannathnettar@yahoo.co.in

1. Introduction

Production of pure, fine and defect free crystals is essential for industrial applications and in the studies of transportation of energy in crystals. Gel technique is a simple and relatively inexpensive method of growing pure crystals at ambient temperatures. Tartrates generally decompose before melting. Single crystals of such materials are conveniently grown using gel diffusion method [1]. Gel technique is also suitable for growing doped, co-doped and metal ion induced crystals [2].

Tartrate crystals exhibit special electrical and optical properties. Tartrate crystals induced with the ions of alkaline earth and transition metals exhibit piezoelectricity, ferroelectricity and dielectric anomalies which are useful in ultrasonic transducers, microphones, linear and nonlinear optical devices [3-6]. Studies on growth and synthesis of strontium tartrate trihydrate and tetrahydrate crystals under distinct growth environments are available in the literature [7-12]. Growth of strontium tartrate pentahydrate using strontium nitrate as a second reactant, and its dielectric studies are also reported [13,14]. Doping of intrinsic crystals help in easily tuning the properties of the lattice to a specific purpose. Effect of the size and chemical nature of dopant particles on various properties, including electrical and optical properties, of crystals has been discussed by Hossain et al. [15].

The present study is mainly focused on the growth of intrinsic strontium L(+) tartrate (IST), Mg^{2+} doped strontium L(+) tartrate (MDST) and Zn^{2+} doped strontium L(+) tartrate (ZDST) crystals, using strontium chloride as a second reactant, with silica hydro gel as the growth medium. Optimal growth condition is established by suitably varying the density of SMS solution, gel pH, concentration and matrix of supernatant solutions. The grown crystals are characterized by spectroscopic and analytical techniques and the results are reported.

2. Material and Methods

Chemicals used to grow IST, MDST and ZDST single crystals are L(+) tartaric acid, strontium chloride ($SrCl_2.6H_2O$), magnesium chloride ($MgCl_2.6H_2O$), zinc chloride ($ZnCl_2$) and sodium meta silicate (SMS) ($Na_2SiO_3.9H_2O$) of AR grade. Silica hydro gel is prepared by mixing SMS solution of specific gravity ranging between 1.035-1.070 gcm^{-3} with 0.5M tartaric acid in the ratio of 5:4. To achieve proper gelling, tartaric acid is added drop wise to SMS solution with constant stirring; the solution is collected in different glass tubes and allowed to set. Chloride solutions of Sr^{2+} ions (3 mL) and Sr^{2+}:Mg^{2+} and Sr^{2+}:Zn^{2+} ions in the ratio of 5:1 are added distinctly in each of the glass tubes over the set gel. Diffusion of cations leads to nucleation with $(C_4H_4O_6)^{2-}$ ions to establish the growth of IST, MDST and ZDST crystals. Growth accomplishes in about 15 days and the crystals are extracted. Following chemical reactions describe the formation of IST, MDST and ZDST crystals, respectively:

Table 1: Growth parameters of IST, MDST and ZDST crystals.

Parameters	IST	MDST	ZDST
SMS specific gravity (gcm^{-3})	1.05	1.055	1.0575
Gel pH	4.00	4.20	4.30
gel temperature (°C)	23.5	23.5	23.5
SMS: Tartaric acid	5 : 4	5 : 4	5 : 4
Reactants ratio	$SrCl_2$	$SrCl_2$:$MgCl_2$ 5 : 1	$SrCl_2$:$ZnCl_2$ 5 : 1
Reactants concentration (M)	0.5	0.5	0.5
Duration of growth	12 days	14 days	15 days
Color	Lemon yellow	Yellow	Yellow
Size $l \times b \times h$ (mm^3)	7.2× 2.8× 1.3	5.0× 1.9× 1.5	3.3× 2.1× 1.6
Morphology	Cylindrical hard and transparent	Hillocky pyramidal, hard and transparent	Hillocky pyramidal, hard and transparent

$$SrCl_2.6H_2O+C_4H_6O_6 \rightarrow SrC_4H_4O_6.5H_2O+2HCl+H_2O$$

$$MgCl_2.6H_2O+SrCl_2.6H_2O+C_4H_6O_6 \rightarrow MgSrC_4H_4O_6.5H_2O+4HCl+6H_2O+½O_2.$$

$$ZnCl_2+SrCl_2.6H_2O+C_4H_6O_6 \rightarrow ZnSrC_4H_4O_6.5H_2O+4HCl+½O_2.$$

The extracted crystals are shown in Figure 1. Table 1 records growth parameters of the grown crystals.

Figure 1. The extracted IST, MDST and ZDST crystals

3. Characterization

Gel pH is optimized using digital pH meter EQ-614A (QUIP-TRONIC). Chemical constituents, cationic distribution and surface morphology of IST, MDST and ZDST crystals are identified using CARL ZIESS FESEM (Oxford instruments) attached with EDS system [16]. Functional group identification of intrinsic and doped crystals is made using FTIR (Fourier transform infrared) spectrophotometer (Bruker -Alpha) by adopting KBr pellet technique in the wave number range 400-4000 cm^{-1} [1,17]. Laser Raman spectroscopic (Raman) measurements are made using Raman microscope: Horiba scientific Xplora Plus, with 532 nm laser source. Thermal stability and decomposition behaviors of the grown crystals are investigated using TG-DSC Simultaneous thermal analyzer (NETZSCH STA 2500A-0027-N) instrument at temperatures in the range of 30-1000 ^oC, with a heating rate of 3 ^oC/min [18].

4. Result and discussion

The EDAX spectra of the crystals, shown in Figure 2, Figure 3 and Figure 4 confirm the presence of Sr^{2+}, Mg^{2+} and Zn^{2+} ions in the crystal geometry. The characteristic peaks in the spectra identify presence of Sr, C and O as prime elements in IST crystal; Mg, Sr, C and O in MDST crystal and Zn, Sr, C and O in ZDST crystal. Table 2 shows the atomic and weight percentages of prime constituents of parent and doped crystals.

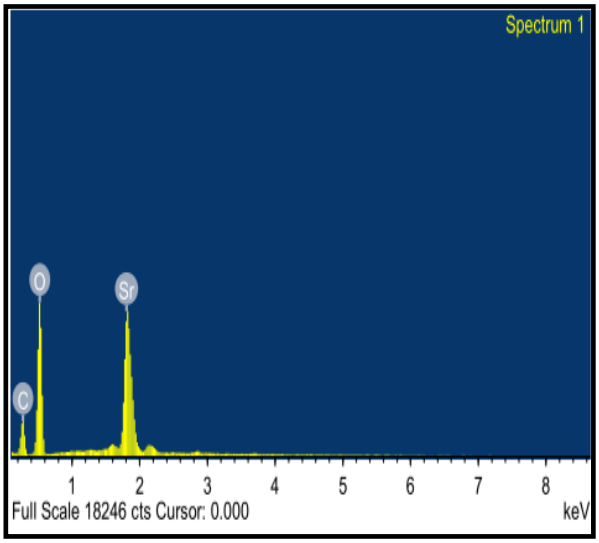

Figure 2: EDAX spectrum- IST crystal

From EDAX measurements, MDST and ZDST crystals are found to have cationic distributions of Sr^{2+}:Mg^{2+}=768:1 and Sr^{2+}:Zn^{2+}=140:1 respectively.

SEM images with 100µm resolution (Figures 5, 6 and 7) show fine morphology of the crystals. Both the parent and doped crystals show good surface finish. MDST and ZDST crystals possess hillocks [19] with sharp pointed tip.

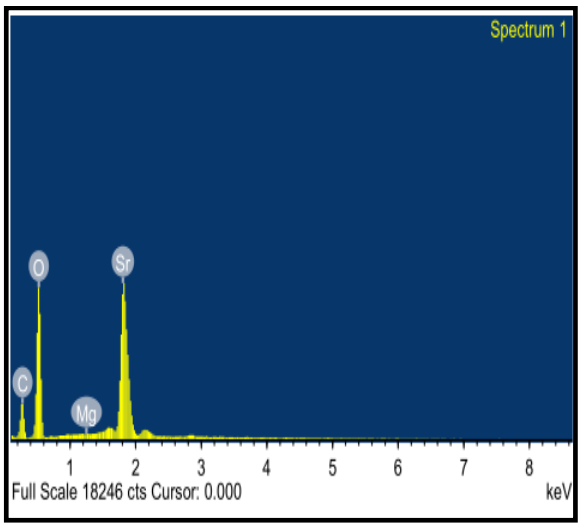

Figure 3: EDAX spectrum-MDST crystal

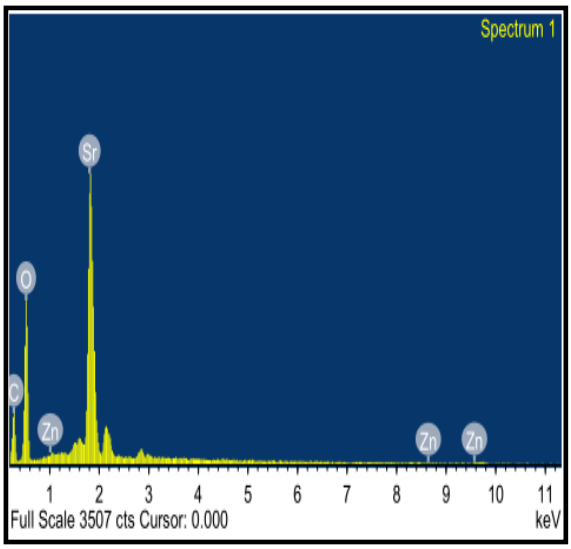

Figure 4: EDAX spectrum- ZDST crystal

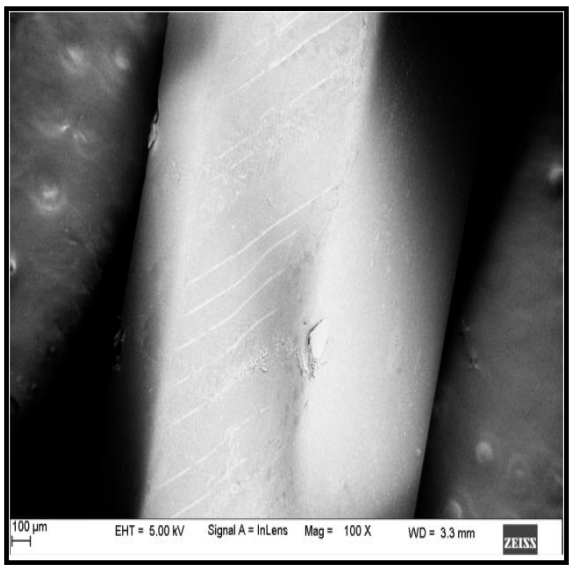

Figure 5: SEM image of IST crystal

Table 2: Atomic and weight percentages of constituent elements.

Crystal	Parameter	Elements				
		O	Mg	Zn	Sr	C
IST	Weight %	49.86	—	—	31.42	18.72
	Atomic %	61.92	—	—	07.12	30.96
MDST	Weight %	48.72	00.01	—	32.99	18.28
	Atomic %	61.58	00.01	—	07.62	30.79
ZDST	Weight %	41.34	—	00.22	42.92	15.52
	Atomic %	59.14	—	00.08	11.21	29.57

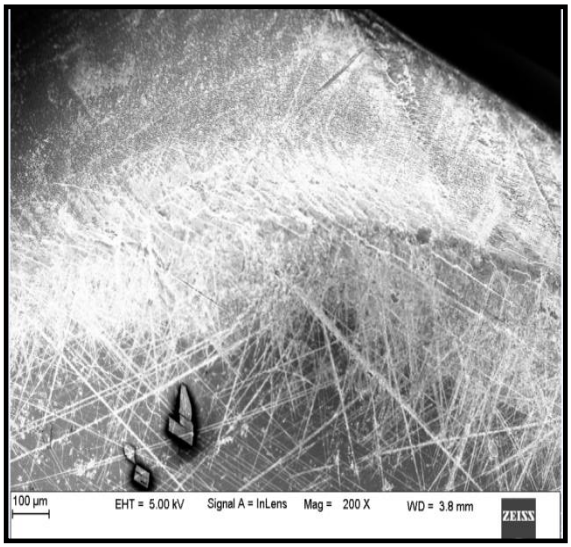

Figure 6: SEM image of MDST crystal

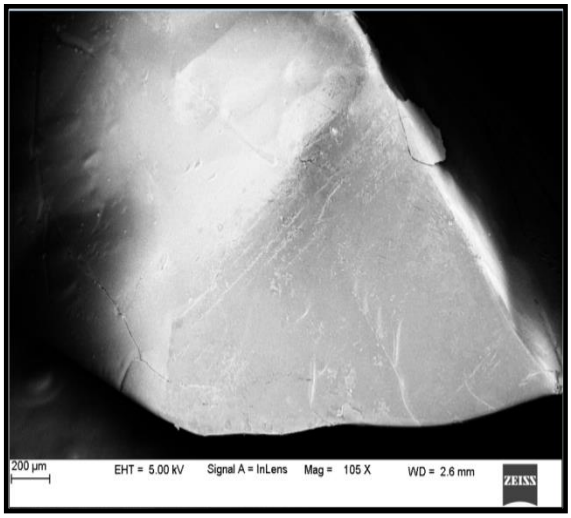

Figure 7: SEM image of ZDST crystal

Following Ben et al [20], various functional groups and the possible stretching modes of the crystals are studied using FTIR and Raman spectra (Figures 8, 9 and 10). The observed wavenumbers and the band assigned are the same in both FTIR and Raman spectra.

In Figure 8, Figure 9 and Figure 10, the functional group region is located above 1600 cm^{-1} and finger print region below this wavenumber [21]. The FTIR profiles of parent and doped crystals followed by Raman spectral results are reported in Table 3, Table 4 and Table 5 (along with relevant references), respectively.

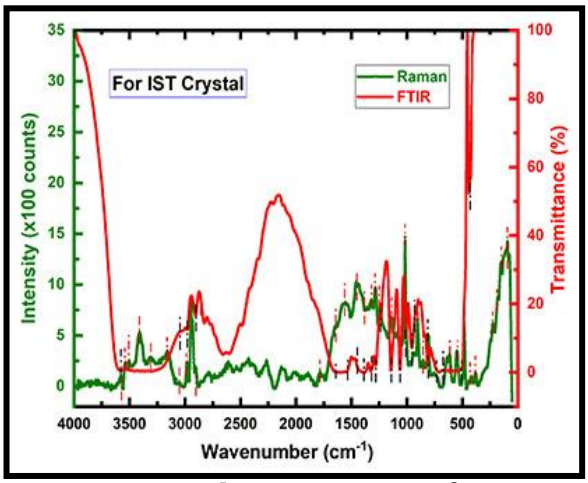

Figure 8: FTIR and Raman spectra of IST crystal

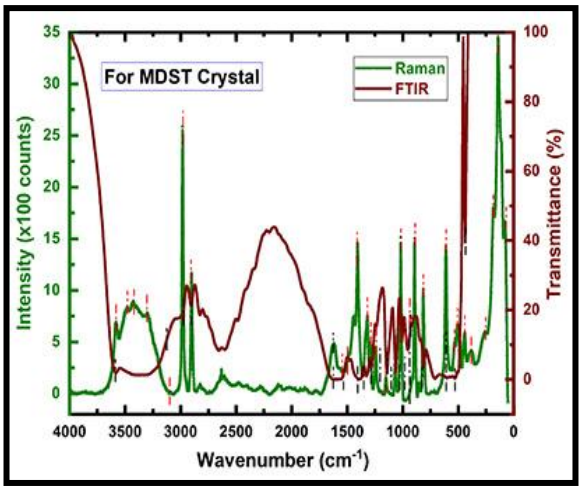

Figure 9: FTIR and Raman spectra of MDST crystal

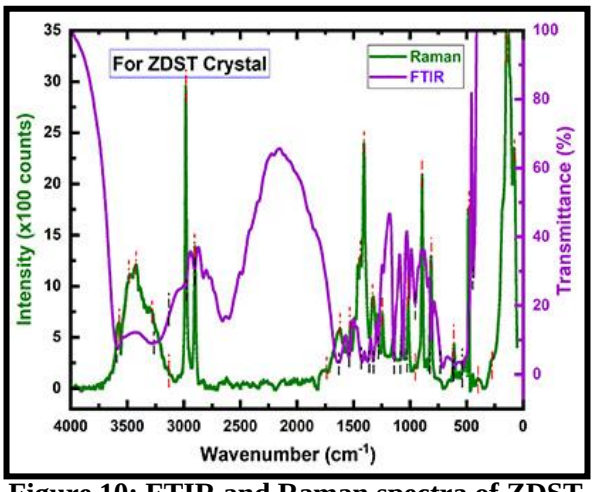

Figure 10: FTIR and Raman spectra of ZDST crystal

The FTIR results reveal that the cationic induction of Mg^{2+} and Zn^{2+} ions results in shifting of the absorption peaks, keeping the functional groups of the parent IST crystal preserved. The molecular vibrations characterized by Raman techniques are in agreement with FTIR results of the crystals.

Table 3: Inference on IST crystals from the spectra shown in Figure 8

FTIR absorption band/peaks (cm^{-1})	**Raman emission band/peaks (cm^{-1})**	**Assignments**	**Reference**
3580–3044	3580, 3537, 3503, 3407, 3300, 3155, 3044	O−H stretch $\nu_1(H_2O)$, $\nu_3(H_2O)$	[22, 23]
2981, 2903	2981, 2947, 2903	C−H stretch	[17, 20, 23 27]
–	1780	C=O stretch	[20, 22, 27, 28]
1650	1650	$\nu_2(H_2O)$	[23]
1557	1557	COO^- asymmetric stretch	[17, 20, 23, 25, 29, 30]
1455	1455	COO^- symmetric stretch	[17, 20, 23, 25, 29, 30]
1393	1393, 1359	O−H bending and deformation	[17, 20, 23, 25]
1320, 1277, 1233	1325, 1277, 1233	C−H bend	[17, 20, 23]
1141, 1060	1136, 1078	C−O symmetric stretch	[17, 20, 22, 23]
1005, 953, 904	1005, 942, 904	C−C symmetric stretch	[1, 13, 25, 29]
812, 610	803, 610	COO^- deformation	[20, 23]
546, 488, 436	546, 488, 436	Metal-oxygen bond	—
—	382, 226, 190, 151, 92	Skeletal deformation COO^- twist and C-C torsion	[17, 20, 23]

Table 4: Inference on MDST crystals from the spectra shown in Figure 9.

FTIR absorption band/peaks (cm^{-1})	**Raman emission band/peaks (cm^{-1})**	**Assignments**	**Reference**
3580–3131	3580, 3480, 3421, 3290, 3131	O−H stretch $\nu_1(H_2O)$, $\nu_3(H_2O)$	[22, 23]
2981, 2898	2981, 2898	C−H stretch	[17, 20, 23–27]
–	1780	C=O stretch	[20, 22, 27, 28]
1615	1615	$\nu_2(H_2O)$	[23]
1543, 1485	1543, 1485	COO^- asymmetric stretch	[17, 20, 23, 25, 29, 30]
1442	1422	COO^- symmetric stretch	[17, 20, 23, 25, 29, 30]
1398	1403	O−H bending and deformation	[17, 20, 23, 25]
1315, 1287, 1238	1315, 1287, 1238	C−H bend	[17, 20, 23]
1142, 1062	1142, 1062	C−O symmetric stretch	[17, 20, 22, 23]
1015, 948	1015, 948, 894	C−C symmetric stretch	[1, 13, 25, 29]
812, 609	812, 609	COO^- deformation	[20, 23]
536, 503, 442	536, 503, 442	Metal-oxygen bond	—
—	382, 253, 184, 140, 77	Skeletal deformation COO^- twist and C-C torsion	[17, 20, 23]

Table 5: Inference for ZDST crystals from the spectra shown in Figure 10

FTIR absorption band/peaks (cm^{-1})	Raman emission band/peaks (cm^{-1})	Assignments	Reference
3580–3131	3581, 3474, 3421, 3295, 3277, 3131	O−H stretch $\nu_1(H_2O)$, $\nu_3(H_2O)$	[22,23]
2981, 2903	2981, 2903	C−H stretch	[17,20,23–27]
–	1742	C=O stretch	[20,22,27,28]
1630	1620	$\nu_2(H_2O)$	[23]
1538	1529	COO^- asymmetric stretch	[17,20,23,25,29,30]
1427	1446	COO^- symmetric stretch	[17,20,23,25,29,30]
1380	1403	O−H bending and deformation	[17,20,23,25]
1320, 1282, 1238	1320, 1282, 1238	C−H bend	[17,20,23]
1146, 1064	1146, 1064	C−O symmetric stretch	[17,20,22,23]
1013, 958	1010, 958, 895	C−C symmetric stretch	[1,13,25,29]
812, 609	812, 609	COO^- deformation	[20,23]
536, 507,447	536, 507, 447	Metal-oxygen bond	—
—	399, 275, 140, 77	Skeletal deformation COO^- twist and C-C torsion	[17,20,23]

TGA and DSC profiles of the IST, MDST and ZDST crystals are shown in Figure 11, Figure 12 and Figure 13 respectively. Both parent and doped crystals show four stages of decomposition.

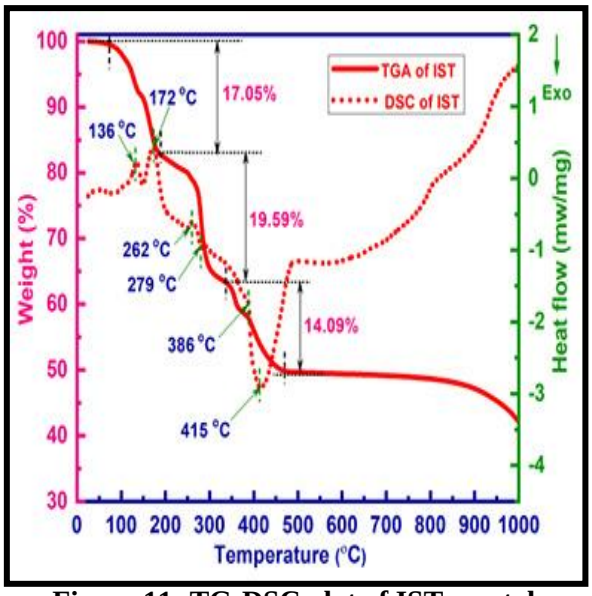

Figure 11: TG-DSC plot of IST crystal

The parent IST crystal exhibits first stage of decomposition (Figure 11) at temperature range 73-190 °C. In this stage, the crystal undergoes a weight loss by 17.05% (calc. loss 16.59%) with the elimination of three water molecules. This corresponds to DSC endothermic peaks at 136 °C and 172 °C. The second stage of decomposition occurs at 190-335 °C, showing weight loss of 19.59% (calc. loss 20.27%), with the elimination of two coordinated water molecules and with liberation of formaldehyde gas. [31]. In the third phase, (temperature range: 335-470 °C), the crystal suffers a weight loss of 14.09% (calc. loss 14.13%) due to the loss of a water molecule and liberation of carbon monoxide. This process results in the formation of strontium oxalic anhydride and the state continues upto 836 °C. During the fourth and final stage of decomposition (temperature range: 836-1000 °C), the crystal is decomposed to strontium oxide (SrO) with liberation of two molecules of carbon monoxide [31].

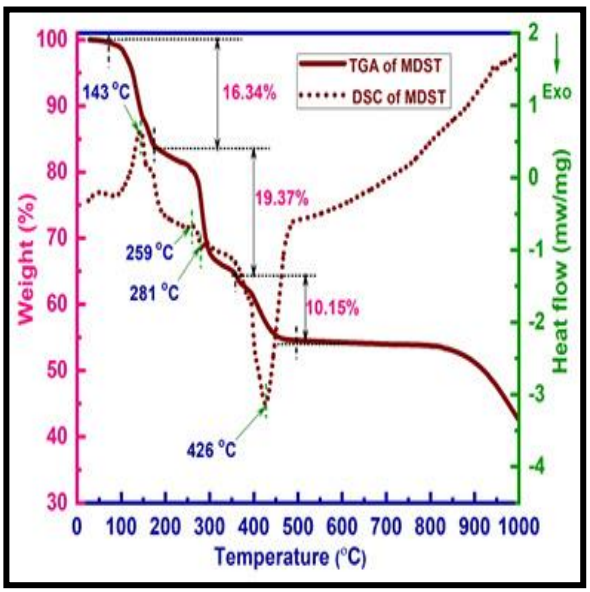

Figure 12: TG-DSC plot of MDST crystal

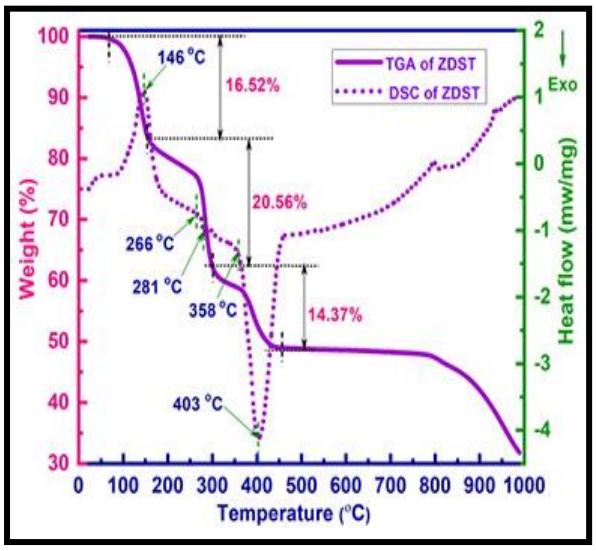

Figure 13: TG-DSC plot of ZDST crystal

The first stage of decomposition of MDST crystal (Figure 12) occurs in the temperature range of 72-176 °C with a weight loss of 16.34% (calc. loss 16.59%), and with the elimination of three water molecules. This corresponds to a DSC endothermic peak at 143 °C. In the second stage of decomposition (temperature range: 176-361 °C), the crystal loses two coordinated water molecules and a molecule of carbon monoxide, undergoing a weight loss of 19.37% (calc. loss 19.66%), attaining stability at strontium magnesium tartronate state. In the third stage (between 361-496 °C), the crystal suffers a weight loss of 10.15% (calc. loss 9.83%) with the liberation of methanol gas (exothermic peak at 426 °C) and forms strontium magnesium oxalate. This state continues up to 812 °C. During the final stage of decomposition (temperature range: 812-1000 °C), the material reduces to strontium magnesium carbonate ($SrMgCO_3$) with liberation of a molecule of carbon monoxide [1, 12, 32].

Figure 13 shows TG-DSC plot for the ZDST crystal. The crystal exhibits four distinct stages of decomposition. The first stage of decomposition, occurring in the range of 65-150 °C, shows a weight loss of 16.52% (calc. loss of 16.59%). This is due to elimination of three lattice water molecules.

In the second stage of decomposition (150-299 °C), the crystal loses two coordinated water molecules along with an exothermic liberation of H_2CO gas, suffering a weight loss of 20.56% (calc. loss 20.28%). In the third stage (299-454 °C), the crystal decomposes to strontium zinc oxalic anhydride unveiling a weight loss of 14.37% (calc. loss 14.13%). This is due to endothermic expelling of H_2O molecules (DSC peak at 358 °C) along with exothermic liberation of a molecule of CO (403 °C) [31]. In the final phase (761-1000 °C), the ZDST crystal loses two molecules of carbon monoxide and attains stability as strontium zinc oxide (SrZnO) [31].

It is evident that the IST and ZDST crystals decompose to oxide state with liberation of 2CO, whereas the MDST crystal lattice attains carbonate state with liberation of a molecule of CO. Thus, at high temperatures, all the crystals exhibit thermal stability. The results of this study also reveal the presence of five water molecules in each of the grown crystal lattice.

The range of temperature, loss of weight and the relevant chemical reaction associated with every stage of decomposition of the crystals are shown in Table 6 and Table 7.

Table 6: Decomposition process of IST, MDST and ZDST crystals.

Crystals	Stages	Temp. range (°C)	Obsrvd. weight loss (%)	Calc. weight loss (%)	Relevant chemical reactions
IST	I	73–190	17.05	16.59	$SrC_4H_4O_6 \cdot 5\,H_2O \longrightarrow SrC_4H_4O_6 \cdot 2\,H_2O + 3\,H_2O$
	II	190–335	19.59	20.27	$SrC_4H_4O_6 \cdot 2\,H_2O \longrightarrow SrC_3H_2O_5 + 2\,H_2O + H_2CO$
	III	335–470	14.09	14.13	$SrC_3H_2O_5 \longrightarrow SrC_2O_3 + H_2O + CO$
	IV	836–1000	—	—	$SrC_2O_3 \longrightarrow SrO + 2\,CO$
MDST	I	72–176	16.34	16.59	$Sr_{0.9987}\,Mg_{0.0013}\,C_4H_4O_6 \cdot 5\,H_2O \longrightarrow Sr_{0.9987}\,Mg_{0.0013}\,C_4H_4O_6 \cdot 2\,H_2O + 3\,H_2O$
	II	176–361	19.37	19.66	$Sr_{0.9987}\,Mg_{0.0013}\,C_4H_4O_6 \cdot 2\,H_2O \longrightarrow Sr_{0.9987}\,Mg_{0.0013}\,C_3H_4O_5 + 2\,H_2O + CO$
	III	361–496	10.15	9.83	$Sr_{0.9987}\,Mg_{0.0013}\,C_3H_4O_5 \longrightarrow Sr_{0.9987}\,Mg_{0.0013}\,C_2O_4 + H_4CO$
	IV	812–1000	—	—	$Sr_{0.9987}\,Mg_{0.0013}\,C_2O_4 \longrightarrow Sr_{0.9987}\,Mg_{0.0013}\,CO_3 + CO$
ZDST	I	65–150	16.52	16.59	$Sr_{0.9929}\,Zn_{0.0071}\,C_4H_4O_6 \cdot 5\,H_2O \longrightarrow Sr_{0.9929}\,Zn_{0.0071}\,C_4H_4O_6 \cdot 2\,H_2O + 3\,H_2O$
	II	150–299	20.56	20.28	$Sr_{0.9929}\,Zn_{0.0071}\,C_4H_4O_6 \cdot 2\,H_2O \longrightarrow Sr_{0.9929}\,Zn_{0.0071}\,C_3H_2O_5 + 2\,H_2O + H_2CO$
	III	299–454	14.37	14.13	$Sr_{0.9929}\,Zn_{0.0071}\,C_3H_2O_5 \longrightarrow Sr_{0.9929}\,Zn_{0.0071}\,C_2O_3 + H_2O + CO$
	IV	761–1000	—	—	$Sr_{0.9929}\,Zn_{0.0071}\,C_2O_3 \longrightarrow Sr_{0.9929}\,Zn_{0.0071}\,O + 2\,CO$

The TG-DSC plots (Figures 11, 12 and 13) clearly highlight the distinct decomposition behaviour of the parent IST and doped MDST and ZDST crystals. The variation in decomposition temperatures, changes in DSC peaks and metastabilities confirm the distinctness among the IST, MDST and ZDST lattices.

Table 7: DSC profile of IST, MDST and ZDST crystals.

Crystal Lattice	DSC Peak Temperature (°C)	Reaction Type(s)
IST	136, 172	Endo
	262, 279	Endo, Exo
	386, 415	Endo, Exo
MDST	143	Endo
	259,281	Endo, Exo
	426	Exo
ZDST	146	Endo
	266,281	Endo, Exo
	358, 403	Endo, Exo

From the EDAX measurements followed by evaluation from FTIR and TG analysis, the estimated chemical formula for the IST crystal is $SrC_4H_4O_6.5H_2O$ with a molecular weight of 325.77. Doping of Mg^{2+} into Sr^{2+} vacancies forms MDST crystals having a chemical formula of $Sr_{0.9987}Mg_{0.0013}C_4H_4O_6.5H_2O$ with a molecular weight of 325.69. Similarly, doping with Zn^{2+} produces ZDST crystals having a chemical formula of $Sr_{0.9929}Zn_{0.0071}C_4H_4O_6.5H_2O$ with a molecular weight of 325.61.

5. Conclusion

MDST and ZDST single crystals are grown by doping a grown IST lattice with Mg^{2+} and Zn^{2+} ions, by adopting gel method in an optimized growth environment. The growth kinetics and morphology of IST, MDST and ZDST crystals are observed to be different. Stoichiometric composition and cationic distribution of the grown crystals are analyzed by EDAX measurements. IST crystals are found to possess a chemical formula $SrC_4H_4O_6.5H_2O$ with a molecular weight of 325.77. MDST crystals show up with a chemical formula of $Sr_{0.9987}Mg_{0.0013}C_4H_4O_6.5H_2O$ (molecular weight 325.69) having a cationic distribution ratio: Sr^{2+}:Mg^{2+} = 768:1. The ZDST crystal bears a chemical formula of $Sr_{0.9929}Zn_{0.0071}C_4H_4O_6.5H_2O$ (molecular weight 325.61) with a cationic distribution ratio: Sr^{2+}:Zn^{2+} = 140:1. All the crystals are pentahydrated. During the final stage of decomposition at high temperatures (761-1000 ^oC), the parent IST and the doped MDST and ZDST crystals attain stable state and exhibit thermal stability indicating usefulness of these crystals in high temperature electronics.

Acknowledgement

The authors are grateful to both the Principal and Head of the department of Physics, FMKMC College, Madikeri, for providing the infrastructure support to this research work.

One of the authors (KBR) acknowledges the help and support given by the faculty members of Department of Science and Technology-Promotion of University Research and Scientific Excellence (DST-PURSE) laboratory, Mangalore University, Mangalore, Center for materials science and technology, Vijnana bhavan, University of Mysore, Mysuru and Department of chemistry, National Institute of Technology, Surathkal (NITK), Mangalore with regard to the elemental analysis (FESEM/EDS), TGA-DSC and FTIR studies of the samples.

Conflict of Interest

The authors declare no conflict of interest

References

[1]. B.S. Kumar, M.R. Kutty, M.S. Kumar and K.R. Babu, Growth and characterization of pure and lithium doped strontium tartrate tetrahydrate crystals by solution-gel technique. *Bulletin of Materials Science*: *30*(4) (2007) 349-355. https://doi.org/10.1007/s12034-007-0058-x

[2]. H.J. Nickl and H.K. Henisch, Growth of calcite crystals in gels. *Journal of the Electrochemical Society: 116*(9) (1969) 1258. https://doi.org/10.1149%2F1.2412292

[3]. Fousek, L.E. Cross and K. Seely, Some properties of the ferroelectric lithium thallium tartrate. *Ferroelectrics*: *1*(1) (1970) 63-70. https://doi.org/10.1080/00150197008237671

[4]. M.E. Torres, T. Lopez, J. Peraza, J. Stockel, A. C. Yanes, C. Gonzalez-Silgo, C. Ruiz-Perez and P. A. Lorenzo-Luis, Structural and dielectric characterization of cadmium tartrate. *Journal of applied physics: 84*(10) (1998) 5729-5732. https://doi.org/10.1063/1.368863

[5]. Ivanov and R. Nikolaj, Dielectric and crystal-optic properties of lithium ammonium tartrate mono-hydrate ferro-elastic crystal under mechanic stress: Piezo-dielectric and piezooptic effects at the phase transition. *Ferroelectrics letters section*: *2*(1) (1984) 45-49. https://doi.org/10.1080/07315178408202433

[6]. F. Jona and G. Shirane, "Ferroelectric Crystals", Dover Publications, Inc, New York, 1993. Chapter VII.

[7]. G.K. Ambady, The crystal and molecular structures of strontium tartrate trihydrate and calcium tartrate tetrahydrate. *Acta Crystallographica Section B: Structural Crystallography and Crystal Chemistry*: *24*(11) (1968) 1548-1557. https://doi.org/10.1107/S0567740868004619

[8]. S.K. Arora, Vipul Patel, Anjana Kothari and Brijesh Amin, Gel growth and preliminary characterization of

strontium tartrate trihydrate. *Crystal growth & design:* *4*(2) (2004) 343-349. https://doi.org/10.1021/cg030024s

[9]. H.K. Hektisch, J. Dennis, and J. I. Hanoka, Crystal growth in gels. *Journal of Physics and Chemistry of Solids*: *26*(3) (1965) 493-496. https://doi.org/10.1016/0022-3697 (65)90123-X

[10]. Bohandy, Joseph and C. John Murphy, An X-ray study of gel-grown strontium tartrate tetrahydrate. *Acta Crystallographica Section B: Structural Crystallography and Crystal Chemistry*: *24*(2) (1968) 286-287. https://doi.org/10.1107/S0567740868002141

[11]. A.R. Patel and S. K. Arora, Growth of strontium tartrate tetrahydrate single crystals in silica gels. *Journal of Materials Science*: *11*(5) (1976) 843-846. https://doi.org/10.1007/BF00542299

[12]. M.H. Rahimkutty, K. Rajendra Babu, K. Sreedharan Pillai, M. R. Sudarsana Kumar and C. M. K. Nair, Thermal behaviour of strontium tartrate single crystals grown in gel. *Bulletin of Materials Science*, *24*(2), (2001) 249-252. https://doi.org/10.1007/BF02710110

[13]. A. Firdous, I. Quasim, M.M. Ahmad and P.N. Kotru, Growth and characterization of strontium tartrate pentahydrate crystals. *Crystal Research and Technology: Journal of Experimental and Industrial Crystallography*: *43*(10) (2008) 1015-1021.https://doi.org/10.1002/crat.200800115

[14]. A. Firdous, I. Quasim, M.M. Ahmad and P.N. Kotru, Dielectric and thermal studies on gel grown strontium tartrate pentahydrate crystals. *Bulletin of Materials Science*: *33*(4) (2010) 377-382.https://doi.org/10.1007/s12034-010-0057-1

[15]. A. Hossain, S. Roy and K. Sakthipandi, The external and internal influences on the tuning of the properties of perovskites: An overview. *Ceramics International*: *45*(4) (2019) 4152-4166. https://doi.org/10.1016/j.ceramint.2018.11.102

[16]. N. Ponnappa, J. Nettar, H. Mylnahalli, D. D'Souza and L. Neratur, Growth, Characterization and Conductivity of Chromium Mixed Cadmium Oxalate Crystals. *Crystal Research and Technology*: *53*(2) (2018) 1700261. https://doi.org/10.1002/crat.201700261

[17]. P. Kolandaivel and S. Selvasekarapandian, FT-IR and Raman Spectra of Ammonium Hydrogen Tartrate and Potassium Hydrogen Tartrate Crystals. *Crystal Research and Technology*: *28*(5) (1993) 665-670. https://doi.org/10.1002/crat.2170280516

[18]. V. Mathivanan, M. Haris and J. Chandrasekaran, Thermal, magnetic, dielectric and anti microbial properties of solution-grown pure and doped sodium potassium tartrate crystals. *Optik*: *127*(4) (2016) 1804-1808. https://doi.org/10.1016/j.ijleo.2015.11.092

[19]. F. Rethinam, Jesu, D. Arivu Oli, S. Ramasamy and P. Ramasamy, Growth and Characterisation of Pure and Nickel-doped Strontium Tartrate Tetrahydrate Single Crystals. *Crystal Research and Technology*: *28*(6) (1993) 861-865. https://doi.org/10.1002/crat.2170280616

[20]. M. Ben Salah, K. Mouaine, P. Becker and C. Carabatos-Nédelec, Single crystal raman scattering, powder infrared spectroscopy and thermal properties of rubidium hydrogen tartrate. *physica status solidi (b)*: *220*(2) (2000) 1025-1032. https://doi.org/10.1002/(SICI) 1521-3951(200008)220:2%3C1025:: AID-PSSB1025%3E3.0.CO;2-5

[21]. B.S. Furniss, A.J. Hannaford, P.W.G. Smith and A.R. Tatchell, Vogel's textbook of practical organic chemistry: ELBS. 1989:1035p.

[22]. L.I. Kozhevina, L.G. Skryabina and Yu K. Tselinskii, The interpretation of the infrared spectrum of tartaric acid. *Journal of Applied Spectroscopy*: *33*(6) (1980) 1347-1351. https://doi.org/10.1007/BF00614043

[23]. N. Kaneko, M. Kaneko and H Takahashi, Infrared and Raman spectra and vibrational assignment of some metal tartrates. *Spectrochimica Acta Part A: Molecular Spectroscopy*: *40*(1) (1984) 33-42. https://doi.org/10.1016/0584-8539(84)80026-4

[24]. X.S, Shajan and C. Mahadevan, On the growth of calcium tartrate tetrahydrate single crystals. *Bulletin of Materials Science*: *27*(4) (2004) 327-331. https://doi.org/10.1007/BF02704767

[25]. H.M. Patil, D.K. Sawant, D.S. Bhavsar, J. H. Patil, and K. D. Girase, FTIR and thermal studies on gel grown neodymium tartrate crystals. *Journal of thermal analysis and calorimetry*: *107*(3) (2012) 1031-1037. https://doi.org/10.1007/s10973-011-1599-1

[26]. D. Lin-Vien, N.B. Colthup, W.G. Fateley and J. G. Grasselli, *The handbook of infrared and Raman characteristic frequencies of organic molecules*. (1991). Elsevier.

[27]. R. Bhattacharjee, Y.S. Jain and H.D. Bist, Laser Raman and infrared spectra of dipotassium tartrate hemihydrate. *Journal of Raman spectroscopy*: *20*(9) (1989) 561-567.https://doi.org/10.1002/jrs.1250200903

[28]. Edsall and T. John, Raman Spectra of Amino Acids and Related Compounds IV. Ionization of Di-and Tricarboxylic Acids. *The Journal of Chemical Physics*: *5*(7) (1937) 508-517. https://doi.org/10.1063/1.1750067

[29]. A.V.R. Warrier and R. S. Krishnan, Infrared spectra of trichloroacetates of copper, calcium, strontium and barium. *Spectrochimica Acta Part A: Molecular Spectroscopy*: *27*(8) (1971) 1243-1246. https://doi.org/10.1016/0584-8539(71)80075-2

[30]. R.R. Kanna, K. Sakthipandi, N. Lenin and E.J.J Samuel, Neodymium doped on the manganese–copper nanoferrites: analysis of structural, optical, dielectric and magnetic properties. *Journal of Materials Science: Materials in Electronics*: *30*(5) (2019) 4473-4486.https://doi.org/10.1007/s10854-019-00736-z

[31]. T. Fukami, S. Tahara, C. Yasuda and K. Nakasone, Crystal Structure and Thermal Properties of SrC4H4O6• 4H2O Single Crystals. *International Research Journal of Pure and Applied Chemistry*: (2016) 1-10. https://doi.org/10.9734/IRJPAC/2016/23674

[32]. S.K. Arora, Vipul Patel and Anjana Kothari, Kinetics and mechanism of thermal decomposition of strontium tartrate crystals. *Materials chemistry and physics*: *84*(2-3) (2004) 323-330. https://doi.org/10.1016/j.matchemphys.2003.10.017